CHAPTER 5

KINEMATICS OF FLUID MOTION

5.1 ELEMENTARY FLOW PATTERNS

Recall the discussion of flow patterns in Chapter 1. The equations for particle paths in a three-dimensional, steady fluid flow are

$$\frac{dx}{dt} = U(\bar{x}) \; ; \qquad \frac{dy}{dt} = V(\bar{x}) \; ; \qquad \frac{dz}{dt} = W(\bar{x}) \, . \tag{5.1}$$

Although the position of a particle depends on time as it moves with the flow, the flow pattern itself does not depend on time and the system (5.1) is said to be *autonomous*. Autonomous systems of differential equations arise in a vast variety of applications in mechanics from the motions of the planets to the dynamics of pendulums to velocity vector fields in steady fluid flow. A great deal about the flow can be learned by plotting the velocity vector field $U_i[\bar{x}]$. When the flow pattern is plotted one notices that among the most prominent features are stagnation points also known as *critical points* that occur where

$$U_i[\bar{x}_c] = 0 \, . \tag{5.2}$$

Quite often the qualitative features of the flow can be almost completely described once the critical points of the flow field have been identified and classified.

5.1.1 LINEAR FLOWS

If the $U_i[\bar{x}]$ are analytic functions of $\bar{x}$, the velocity field can be expanded in a Taylor series about the critical point and the result can be used to gain valuable information about the geometry of the flow field. Retaining just the lowest order term in the expansion of $U_i[\bar{x}]$ the result is a linear system of equations,

$$\frac{dx_i}{dt} = A_{ik}(x_k - x_{kc}) + O((x_k - x_{kc})^2) + \ldots \tag{5.3}$$

where A_{ik} is the gradient tensor of the velocity field evaluated at the critical point and $\bar{x}_c$ is the position vector of the critical point.

$$A_{ik} = \left(\frac{\partial U_i}{\partial x_k}\right)_{\bar{x} = \bar{x}_c} . \tag{5.4}$$

The linear, local solution is expressed in terms of exponential functions and only a relatively small number of solution patterns are possible. These are determined by the invariants of A_{ik}. The invariants arise naturally as traces of various powers of A_{ik}. They are all derived as follows. Transform A_{nm}

$$B_{ik} = M_{in} A_{nm} \overline{M}_{mk} \tag{5.5}$$

where M is a non-singular matrix and $\overline{M}$ is its inverse. Take the trace of (5.5)

$$B_{ii} = M_{in} A_{nm} \overline{M}_{mi} = \overline{M}_{mi} M_{in} A_{nm} = \delta_{mn} A_{nm} = A_{mm} . \tag{5.6}$$

The trace is invariant under the affine transformation M_{ik}. One can think of the vector field, U_i, as if it is imbedded in an n-dimensional block of rubber. An affine transformation is one which stretches or distorts the rubber block without ripping it apart or reflecting it through itself. For traces of higher powers the proof of invariance is similar.

$$tr(B^{\alpha}) =$$
$$M_{jn_1} A_{n_1 m_1} \overline{M}_{m_1 j_1} M_{j_1 n_2} A_{n_2 m_2} \overline{M}_{m_2 j_2} \ldots M_{j_{\alpha-1} n_\alpha} A_{n_\alpha m_\alpha} \overline{M}_{m_\alpha j} = \quad . \tag{5.7}$$
$$= tr(A^{\alpha})$$

The traces of all powers of the gradient tensor remain invariant under affine transformation. Likewise any combination of the traces is invariant.

5.1.2 Linear flows in two dimensions

In two dimensions the eigenvalues of A_{ik} satisfy the quadratic

$$\lambda^2 + P\lambda + Q = 0 \tag{5.8}$$

where P and Q are the invariants

$$P = -A_{ii} \quad ; \qquad Q = Det(A_{ik}) . \tag{5.9}$$

The eigenvalues of A_{ik} are

$$\lambda = -\frac{P}{2} \pm \frac{1}{2}\sqrt{P^2 - 4Q} . \tag{5.10}$$

and the character of the local flow is determined by the quadratic discriminant

$$D = Q - \frac{P^2}{4} . \tag{5.11}$$

The various possible flow patterns can be summarized on a cross-plot of the invariants as shown in Figure 5.1. If $D > 0$ the eigenvalues are complex and a spiraling motion can be expected in the neighborhood of the critical point.

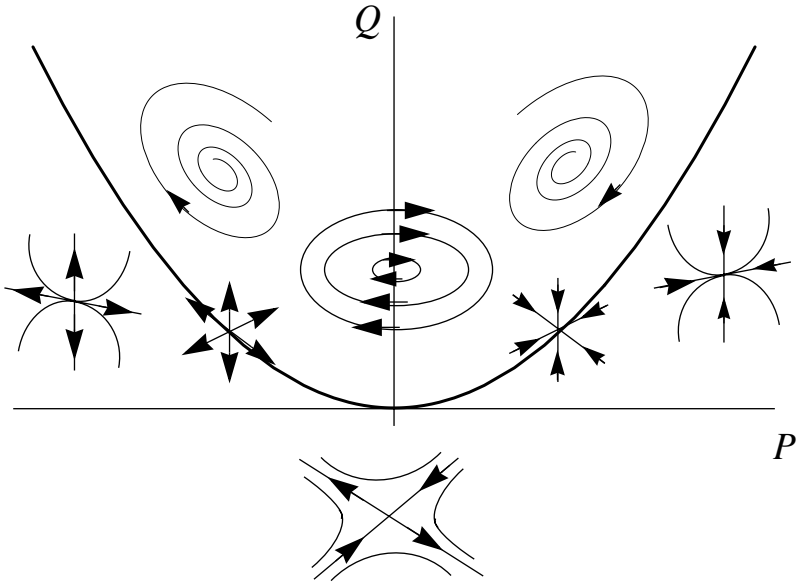

Figure 5.1 Classification of linear flows in two dimensions

Depending on the sign of P the spiral may be stable or unstable (spiraling in or spiraling out). If $D < 0$ the eigenvalues are real and a predominantly straining flow can be expected. In this case the directionality of the local flow is defined by the two eigenvectors of A_{ik}. The case $P = 0$ corresponds to incompressible flow for which there are only two possible kinds of critical points, centers with $Q > 0$ and saddles with $Q < 0$. The line $Q = 0$ in Figure 5.1 corresponds to a degenerate case where (5.8) reduces to $\lambda(\lambda + P) = 0$. In this instance the critical point becomes a line with trajectories converging from either side of the line.

5.1.3 Linear flows in three dimensions

In three dimensions the eigenvalues of A_{ik} satisfy the cubic

$$\lambda^3 + P\lambda^2 + Q\lambda + R = 0 \tag{5.12}$$

where the invariants are

$$\begin{aligned} P &= -tr[\boldsymbol{A}] = -A_{ii} \\ Q &= \frac{1}{2}(P^2 - tr[\boldsymbol{A}^2]) = \frac{1}{2}(P^2 - A_{ik}A_{ki}) \\ R &= \frac{1}{3}(-P^3 + 3PQ - tr[\boldsymbol{A}^3]) = \frac{1}{3}(-P^3 + 3PQ - A_{ik}A_{km}A_{mi}) \end{aligned} \quad . \tag{5.13}$$

Any cubic polynomial can be simplified as follows. Let

$$\lambda = \alpha - \frac{P}{3} \tag{5.14}$$

Then α satisfies

$$\alpha^3 + \hat{Q}\alpha + \hat{R} = 0 \tag{5.15}$$

where

$$\hat{Q} = Q - \frac{1}{3}P^2 \quad ; \qquad \hat{R} = R - \frac{1}{3}PQ + \frac{2}{27}P^3 \tag{5.16}$$

Let

$$a_1 = \left(-\frac{\hat{R}}{2} + \frac{1}{3\sqrt{3}}\left(\hat{Q}^3 + \frac{27}{4}\hat{R}^2\right)^{\frac{1}{2}}\right)^{\frac{1}{3}}; \quad a_2 = \left(-\frac{\hat{R}}{2} - \frac{1}{3\sqrt{3}}\left(\hat{Q}^3 + \frac{27}{4}\hat{R}^2\right)^{\frac{1}{2}}\right)^{\frac{1}{3}} \tag{5.17}$$

The real solution of (5.15) is expressed as.

$$\alpha_1 = a_1 + a_2 \tag{5.18}$$

and the complex (or remaining real) solutions are

$$\begin{aligned} \alpha_2 &= -\frac{1}{2}(a_1 + a_2) + \frac{i\sqrt{3}}{2}(a_1 - a_2) \\ \alpha_3 &= -\frac{1}{2}(a_1 + a_2) - \frac{i\sqrt{3}}{2}(a_1 - a_2) \end{aligned} \tag{5.19}$$

When (5.12) is solved for the eigenvalues one is led to the cubic discriminant

$$D = \frac{27}{4}R^2 + \left(P^3 - \frac{9}{2}PQ\right)R + Q^2\left(Q - \frac{1}{4}P^2\right). \tag{5.20}$$

The surface $D = 0$, is depicted in Figure 5.2 below.

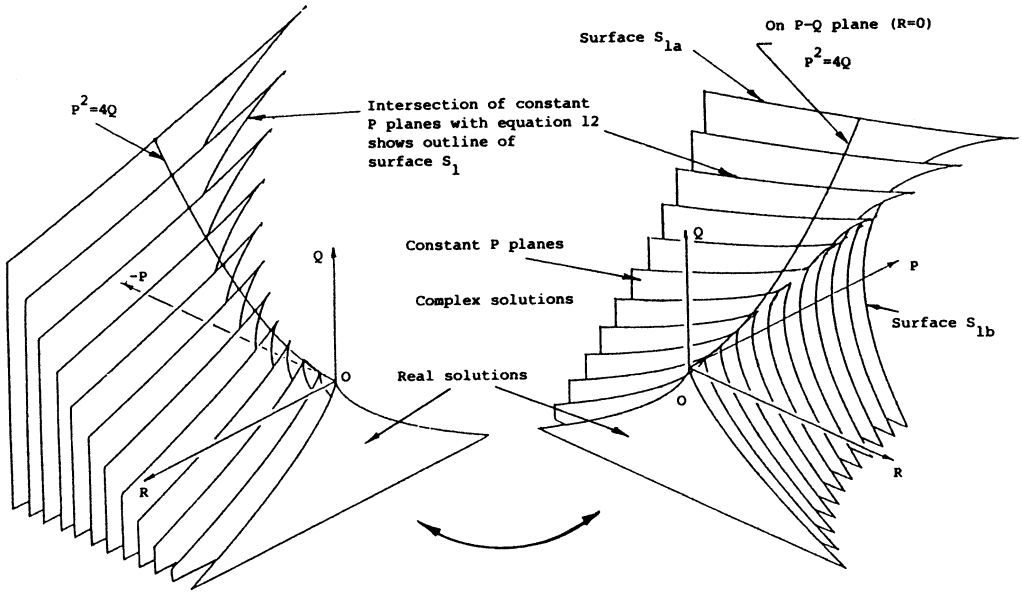

Figure 5.2 The surface dividing real and complex eigenvalues in three dimensions.

To help visualize the surface (5.20) it is split down the middle on the plane $P = 0$ and the two parts are rotated away to provide a better view. Note that (5.20) can be regarded as a quadratic in R and so the surface $D = 0$ is really composed of two roots for R that meet in a cusp. If $D > 0$ the point (P, Q, R) lies above the surface and there is one real eigenvalue and two complex conjugate eigenvalues. If $D < 0$ all three eigenvalues are real.

The invariants can be expressed in terms of the eigenvalues as follows. If the eigenvalues are real,

$$\begin{aligned} P &= -(\lambda^1 + \lambda^2 + \lambda^3) \\ Q &= \lambda^1\lambda^2 + \lambda^1\lambda^3 + \lambda^2\lambda^3 \\ R &= -\lambda^1\lambda^2\lambda^3 \end{aligned} \tag{5.21}$$

and if the eigenvalues are complex

$$\begin{aligned} P &= -(2\sigma + b) \\ Q &= \sigma^2 + \omega^2 + 2\sigma b \\ R &= -b(\sigma^2 + \omega^2) \end{aligned} \tag{5.22}$$

where b is the real eigenvalue and σ and ω are the real and imaginary parts of the complex conjugate eigenvalues.

5.1.4 Incompressible Flow

Flow patterns in incompressible flow are characterized by

$$\nabla \bullet U = \frac{\partial U_i}{\partial x_i} = A_{ii} = 0. \tag{5.23}$$

This corresponds to $P = 0$. In this case the discriminant is

$$D = Q^3 + \frac{27}{4}R^2 \tag{5.24}$$

and the invariants simplify to

$$Q = -\frac{1}{2}A_{ik}A_{ki} \quad , \qquad R = -\frac{1}{3}A_{ik}A_{km}A_{mi}\,. \tag{5.25}$$

The various possible elementary flow patterns for this case can be categorized on a plot of Q versus R shown in Figure 5.3.

.

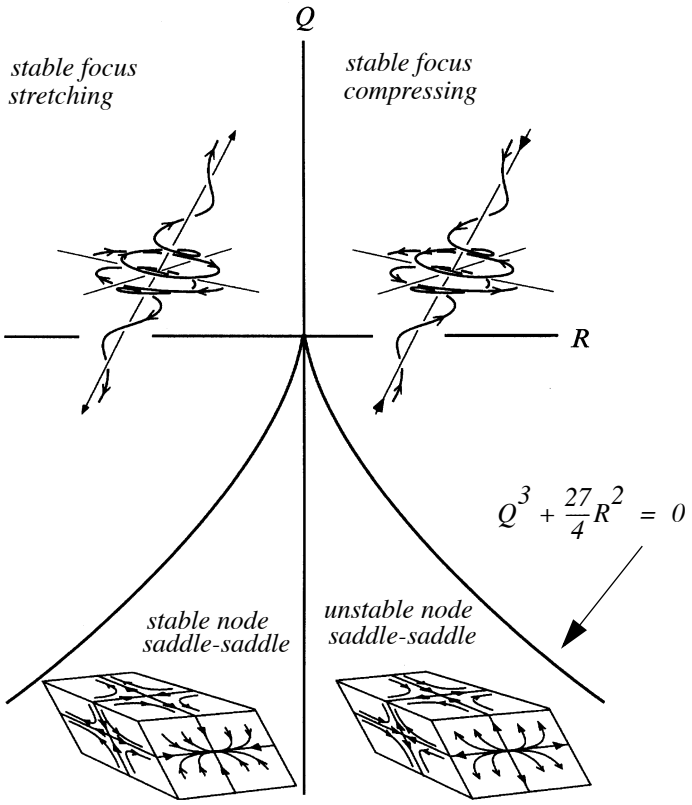

Figure 5.3 Three-dimensional flow patterns in the plane $P = 0$.

Figure 5.1 and Figure 5.3 are cuts through the surface (5.20) at $R = 0$ and $P = 0$ respectively.

5.1.5 FRAMES OF REFERENCE

We introduced the transformation of coordinates between a fixed and moving frame in Chapter 1. Here we briefly revisit the subject again in the context of critical points. For a general smooth flow, the particle path equations (5.1) can be expanded as a Taylor series about any point $\bar{x}_0$ as follows

$$\frac{dx_i}{dt} = U_i\Big|_{\bar{x}=\bar{x}_0} + A_{ik}\Big|_{\bar{x}=\bar{x}_0}(x_k - x_{0k}) + O((x_k - x_{0k})^2) + \ldots . \tag{5.26}$$

If a coordinate system is attached to and moves with the particle at $\bar{x}_0$ with the velocity $U_i\Big|_{\bar{x}=\bar{x}_0}$ so that

$$\begin{aligned} \bar{x}' &= \bar{x} - \bar{x}_0 \\ \overline{U}' &= \overline{U} - \overline{U}\Big|_{\bar{x}=\bar{x}_0} \end{aligned} \tag{5.27}$$

then in that frame of reference the origin of coordinates in effect becomes a critical point (since the velocity is zero there) and the flow pattern that an observer in this coordinate system would see is determined by the second and higher order terms in (5.26).

$$\frac{dx'_i}{dt} = A_{ik}\Big|_{\bar{x}'=0} x'_k + O(x'^2_k) + \ldots . \tag{5.28}$$

The elementary flow patterns described above are what would be seen locally at an instant by an observer moving with a fluid element. Notice that the velocity gradient tensor referred to either frame is the same. In this way the velocity gradient tensor can be used to infer the geometry of the local flow pattern at any point in an unambiguous, frame-invariant manner.

Categorizing flow patterns using the invariants of the velocity gradient tensor has a long history of applications in fluid mechanics particularly in the kinematic description of flow separation and reattachment near a solid surface. More recently these methods have been used to describe light propagation near complex apertures and to describe changes in the electron charge density field in molecules during the making and breaking of chemical bonds.

5.2 RATE-OF-STRAIN AND RATE-OF-ROTATION TENSORS

The velocity gradient tensor

$$A_{ij} = \partial U_i / \partial x_j . \tag{5.29}$$

can be split into a symmetric and antisymmetric part

$$A_{ij} = \frac{\partial U_i}{\partial x_j} = \frac{1}{2}\left(\frac{\partial U_i}{\partial x_j} + \frac{\partial U_j}{\partial x_i}\right) + \frac{1}{2}\left(\frac{\partial U_i}{\partial x_j} - \frac{\partial U_j}{\partial x_i}\right). \tag{5.30}$$

The symmetric part is the rate-of-strain tensor

$$S_{ij} = \frac{1}{2}\left(\frac{\partial U_i}{\partial x_j} + \frac{\partial U_j}{\partial x_i}\right) \tag{5.31}$$

The anti-symmetric part is the rate-of-rotation tensor or spin tensor

$$W_{ij} = \frac{1}{2}\left(\frac{\partial U_i}{\partial x_j} - \frac{\partial U_j}{\partial x_i}\right). \tag{5.32}$$

The vorticity vector $\overline{\Omega} = \nabla \times \overline{U}$ is related to the velocity gradients by

$$\Omega_i = \varepsilon_{ijk}(\partial U_k / \partial x_j) \tag{5.33}$$

and the spin tensor is related to the vorticity by

$$W_{ik} = \frac{1}{2}\varepsilon_{ijk}\Omega_j. \tag{5.34}$$

All local flow patterns can be regarded as a linear sum of a purely rotational motion and a purely straining motion. The balance between these two components determines which of the local flow fields shown in Figure 5.1 or Figure 5.3 will exist at the point. As we move into our studies of compressible flow we shall see that a natural division exists between flows that are irrotational, where the effects of viscosity can often be neglected, and flows that are strain-rate dominated where viscosity plays an important and sometimes dominant role.

5.3 VISCOUS INCOMPRESSIBLE FLOW NEAR A WALL

One of the most important applications of the theory described in this chapter is to the problem of flow separation in two and three dimensions. Particularly in three dimensions, the geometry of the velocity field in separated flows was very poorly understood until the 1960's when a variety of experimental techniques were developed that enabled researchers to visualise the flow very near the surface

of a solid body. When the images from these experiments were analyzed, it quickly became clear that topological methods would be needed to organize and understand the complex patterns that were observed.

Fast forward to today and in many ways we still face the same problem. Computational tools can be used to generate immense masses of data on complex three-dimensional flows including detailed velocity fields. Topological methods are essential to the analysis of the data.

In this section we will examine the viscous flow very near a wall where the no-slip condition applies. The figure below shows the coordinate system. The unit normal vector to the wall is $\bar{n} = (0, 0, n_z) = (0, 0, 1)$.

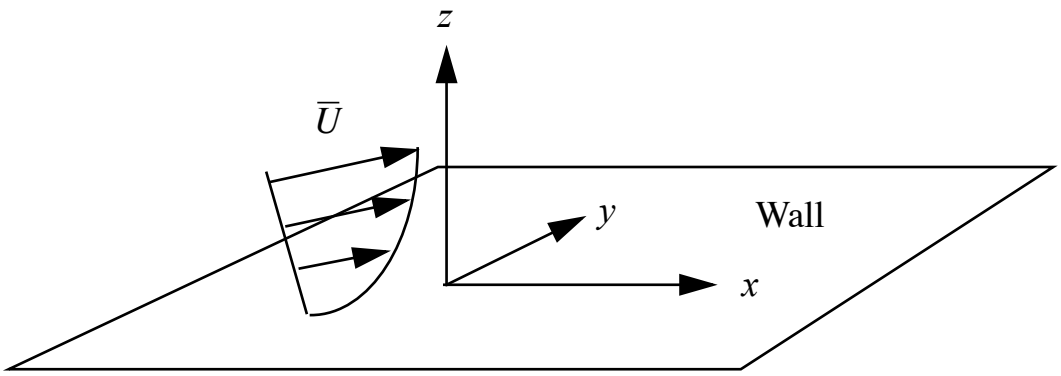

Figure 5.4 Velocity vector above a no-slip wall.

Expand the velocity field (U, V, W) near the wall to second order.

$$
\begin{aligned}
U &= A_{11}x + A_{12}y + A_{13}z + B_{111}x^2 + B_{112}xy + B_{113}xz + B_{122}y^2 + B_{123}yz + B_{133}z^2 \\
V &= A_{21}x + A_{22}y + A_{23}z + B_{211}x^2 + B_{212}xy + B_{213}xz + B_{222}y^2 + B_{223}yz + B_{233}z^2 \\
W &= A_{31}x + A_{32}y + A_{33}z + B_{311}x^2 + B_{312}xy + B_{313}xz + B_{322}y^2 + B_{323}yz + B_{333}z^2
\end{aligned}
\tag{5.35}
$$

Derivatives of the velocity in the (x, y) plane are zero to all orders. Therefore

$$\begin{aligned} A_{11} &= A_{12} = B_{111} = B_{112} = B_{122} = 0 \\ A_{21} &= A_{22} = B_{211} = B_{212} = B_{222} = 0 \\ A_{31} &= A_{32} = B_{311} = B_{312} = B_{322} = 0 \end{aligned} \tag{5.36}$$

The expansion of the velocity field near the wall reduces to

$$\begin{aligned} U &= A_{13}z + B_{113}xz + B_{123}yz + B_{133}z^2 \\ V &= A_{23}z + B_{213}xz + B_{223}yz + B_{233}z^2 \\ W &= A_{33}z + B_{313}xz + B_{323}yz + B_{333}z^2 \end{aligned} \tag{5.37}$$

Apply the continuity equation to (5.37).

(5.38)

$$\frac{\partial U}{\partial x} + \frac{\partial V}{\partial y} + \frac{\partial W}{\partial z} = A_{33} + (B_{113} + B_{223} + 2B_{333})z + B_{313}x + B_{323}y = 0$$

Although z in (5.38) is small, it is essentially arbitrary, as are x and y , and (5.38) can only be satisfied if

$$\begin{aligned} A_{33} &= 0 \\ B_{113} + B_{223} + 2B_{333} &= 0 \\ B_{313} &= B_{323} = 0 \end{aligned} \tag{5.39}$$

Using (5.39) the velocity field reduces further.

$$\begin{aligned} U &= A_{13}z + B_{113}xz + B_{123}yz + B_{133}z^2 \\ V &= A_{23}z + B_{213}xz + B_{223}yz + B_{233}z^2 \\ W &= -\frac{(B_{113} + B_{223})}{2}z^2 \end{aligned} \tag{5.40}$$

The viscous stress tensor also simplifies considerably. At the wall

$$\left.\frac{\tau_{ij}}{\rho}\right|_{z=0} = \nu \begin{bmatrix} 2\frac{\partial U}{\partial x} & \left(\frac{\partial U}{\partial y}+\frac{\partial V}{\partial x}\right) & \left(\frac{\partial U}{\partial z}+\frac{\partial W}{\partial x}\right) \\ \left(\frac{\partial U}{\partial y}+\frac{\partial V}{\partial x}\right) & 2\frac{\partial V}{\partial y} & \left(\frac{\partial V}{\partial z}+\frac{\partial W}{\partial y}\right) \\ \left(\frac{\partial U}{\partial z}+\frac{\partial W}{\partial x}\right) & \left(\frac{\partial V}{\partial z}+\frac{\partial W}{\partial y}\right) & 2\frac{\partial W}{\partial z} \end{bmatrix}_{z=0} = \nu \begin{bmatrix} 0 & 0 & \frac{\partial U}{\partial z} \\ 0 & 0 & \frac{\partial V}{\partial z} \\ \frac{\partial U}{\partial z} & \frac{\partial V}{\partial z} & 0 \end{bmatrix}_{z=0} \tag{5.41}$$

The viscous part of the traction vector on the wall is

$$F_{i_{wall}} = \left.\frac{\tau_{ij}}{\rho} n_j\right|_{z=0} = \nu \begin{bmatrix} 0 & 0 & \frac{\partial U}{\partial z} \\ 0 & 0 & \frac{\partial V}{\partial z} \\ \frac{\partial U}{\partial z} & \frac{\partial V}{\partial z} & 0 \end{bmatrix} \begin{bmatrix} 0 \\ 0 \\ n_z \end{bmatrix} = \nu \begin{bmatrix} \frac{\partial U}{\partial z} n_z \\ \frac{\partial V}{\partial z} n_z \\ 0 \end{bmatrix} = \nu \begin{bmatrix} A_{13} \\ A_{23} \\ 0 \end{bmatrix} = \begin{bmatrix} F_x \\ F_y \\ 0 \end{bmatrix} \tag{5.42}$$

The traction vector on the wall forms a two-dimensional vector field. The velocity field near the wall can now be expressed as

$$\begin{aligned} \frac{U}{z} &= \frac{F_x}{\nu} + B_{113}x + B_{123}y + B_{133}z \\ \frac{V}{z} &= \frac{F_y}{\nu} + B_{213}x + B_{223}y + B_{233}z \\ \frac{W}{z} &= -\frac{(B_{113}+B_{223})}{2}z \end{aligned} \tag{5.43}$$

The surface traction vector field defines limiting streamlines at the wall. At a critical point $(F_x, F_y) = (0, 0)$, and stream lines in the neighborhood of the critical point are determined by a three-dimensional vector field of a particular form.

$$\begin{aligned} \frac{dx}{d\tau} &= B_{113}x + B_{123}y + B_{133}z \\ \frac{dy}{d\tau} &= B_{213}x + B_{223}y + B_{233}z \\ \frac{dz}{d\tau} &= -\frac{(B_{113}+B_{223})}{2}z \end{aligned} \tag{5.44}$$

where $d\tau = zdt$ is a transformed time variable. Equation (5.44) can be used to classify so-called "no-slip' critical points.using the theory discussed above and the roadmap provided by Chong, Perry and Cantwell *Physics of Fluids* A, Vol. 2, No. 6, 1990. The figure below shows a model flow from this paper used to simulate a three-dimensional separation bubble.

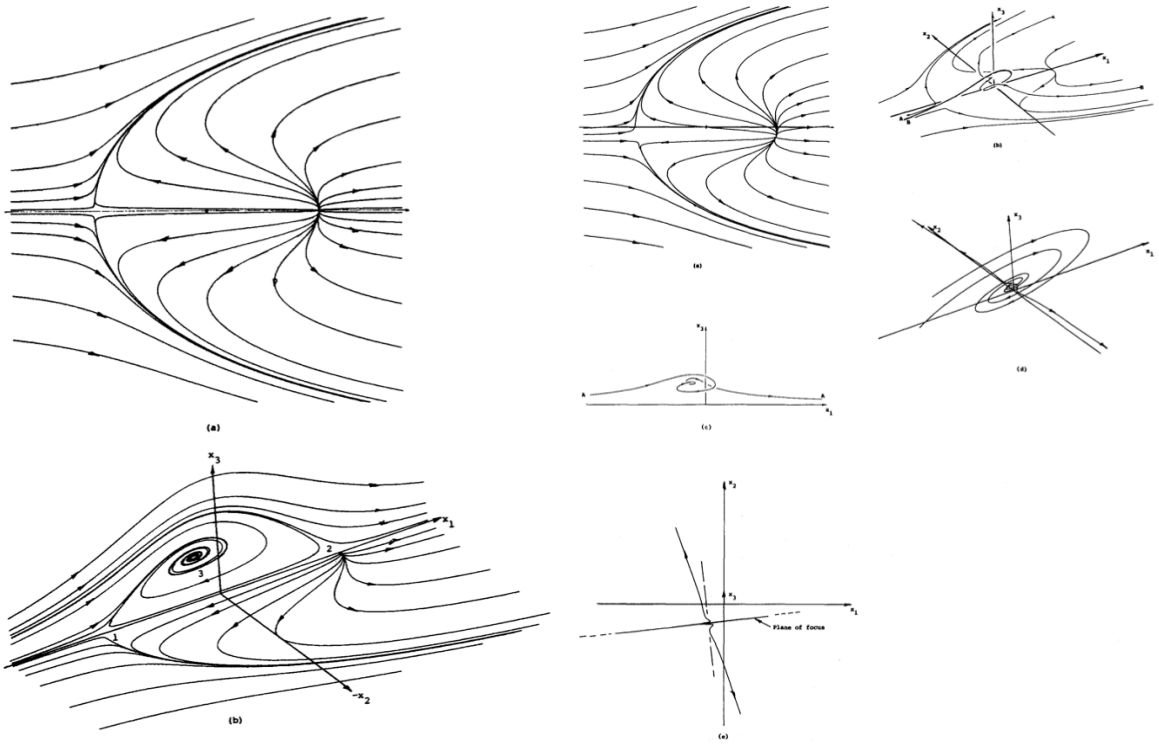

Figure 5.5 Model flow used to study three-dimensional separation. On the left limiting streamlines at the wall are shown with streamlines in a symmetry plane normal to the wall. On the lft a small degree of asymmetry is added to the flow along with depiction of several individual streamlines.

5.3.1 TOPOLOGICAL RULES

The global flow patterns on the surface in which the critical points are imbedded are smooth vector fields subject to certain rules depending on the topological structure of the surface. The most well known rule is the so-called "hairy ball" theorem" that applies to a simply connected three-dimensional body that can be developed into a sphere. If a sphere is covered by hair and all the hairs are combed along the surface from the north pole to the south pole the result would be an unstable node at the north pole and a stable node at the south pole; 2 nodes and

no saddles. If at some point on the sphere one were to gather local vectors into a new node, there would also have to appear a saddle to maintain a topologically consistent vector field with no gaps or tears; 3 nodes and one saddle. It is pretty clear that one cannot add, say a node to the surface flow without also adding a saddle.

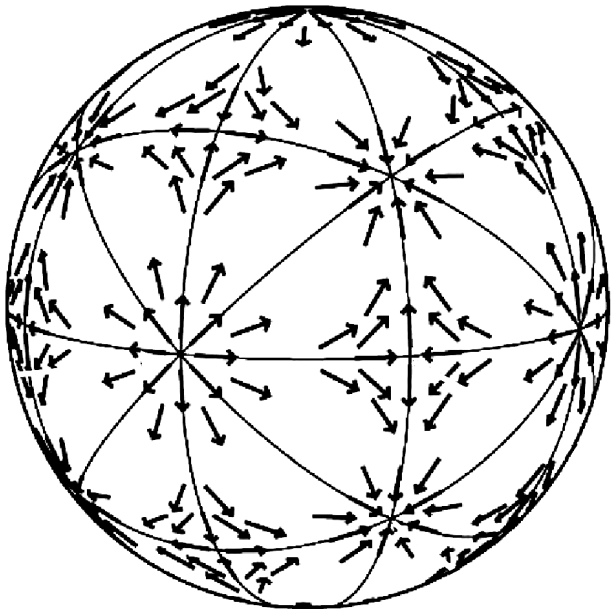

Figure 5.6 Vector field on the surface of a sphere.

Figure 5.6 shows a number of nodes and saddles on a sphere connected by selected streamlines. If the nodes and saddles are counted, the difference is always two regardless of how many critical points are on the surface of the sphere.

1) On a simply connected three-dimensional body

$$\left\{ \sum nodes - \sum saddles \right\} = 2 \tag{5.45}$$

The result (5.45) is specific to a sphere. If the vector field were on the surface of a torus, an object with one hole, the number of nodes and saddles would be the same. This whole subject leads to a major area of mathematics called topology that is concerned with the properties of spaces that remain invariant under continuous deformations.

Tobak and Peake (*Annual Reviews of Fluid Mechanics* 1982) in their review of 3-D separation include a number of additional rules that are useful for interpreting visualization images.

2) On a 3-D body B attached to a plane wall P without gaps that extends to infinity upstream or downstream or is the surface of a torus.

$$\left\{ \sum nodes - \sum saddles \right\}_{P+B} = 0 \tag{5.46}$$

3) Streamlines on a 2-D plane cutting a 3-D body. The count includes half nodes and half saddles attached to the surface of the body.

$$\left\{ \sum nodes + \frac{1}{2} \sum surface\ nodes \right\} - \left\{ \sum saddles + \frac{1}{2} \sum surface\ saddles \right\} = -1 \tag{5.47}$$

4) Streamlines on a vertical plane cutting a surface that extends to infinity upstream and downstream. See Figure 5.5 for an example with two half saddles on the wall and a single focal node off the surface in the cutting plane.

$$\left\{ \sum nodes + \frac{1}{2} \sum surface\ nodes \right\} - \left\{ \sum saddles + \frac{1}{2} \sum surface\ saddles \right\} = 0 \tag{5.48}$$

5) Streamlines on the projection onto a spherical surface of a conical flow past a 3-D body.

$$\left\{ \sum nodes + \frac{1}{2} \sum surface\ nodes \right\} - \left\{ \sum saddles + \frac{1}{2} \sum surface\ saddles \right\} = 0 \tag{5.49}$$

5.3.2 A SUCCESSFUL APPLICATION

During flight testing of the Boeing 767 in 1985 there was a problem with 3-D separation over the wing upper surface behind the engine nacelle during high angle-of-attack operations. This problem led to a significant loss of lift and poor low speed performance.

The problem was studied using oil flow visualization and it was decided to add a large vortex generator to the inboard side of the engine nacelle to control the separation. The chine vortex reattaches the flow over the wing and recovers the lost

lift during low-speed, high-angle-of-attack flight. This device reduced the approach speed of the B767 by 5 knots and the landing distance by 250 feet. It is used by the B767 and the B737-400.

The condensation at the low pressure (low temperature) center of the chine vortex is easily visible from a window seat on a humid day.

Figure 5.7 Condensation reveals the core of a chine vortex.

The theory described in this chapter finds a wide variety of applications to flow separation about aircraft, automobiles, trucks, and buildings as well geophysical flows and convective mixing of scalars in the built environment.

5.4 PROBLEMS

Problem 1 - The simplest 2-D flows imaginable are given by the linear system

$$\begin{aligned} \frac{dx}{dt} &= ax + by \\ \frac{dy}{dt} &= cx + dy \end{aligned} \tag{5.50}$$

Sketch the corresponding flow pattern for the following cases

i) $(a, b, c, d) = (1, -1, -1, -1)$

ii) $(a, b, c, d) = (1, -3, 1, -1)$

iii) $(a, b, c, d) = (-1, 0, 0, -1)$

Work out the invariants of the velocity gradient tensor as well as the various components of the rate-of-rotation and rate-of-strain tensors and the vorticity vector. Which flows are incompressible?

Problem 2 - An unforced damped pendulum is governed by the second order ODE

$$\frac{d^2\theta}{dt^2} + \beta\frac{d\theta}{dt} + \frac{g}{L}Sin(\theta) = 0 \tag{5.51}$$

Let $x = \theta(t)$ and $y = d\theta/dt$. Use these variables to convert the equation to the canonical form.

$$\begin{aligned} \frac{dx}{dt} &= U(x, y) \\ \frac{dy}{dt} &= V(x, y) \end{aligned} \tag{5.52}$$

Sketch the "streamlines" defined by (5.52). Locate and categorize any critical points according methods developed in this chapter. Identify which points are dominated by rotation and which are dominated by the rate-of-strain. You can do this graphically by drawing line segments of the appropriate slope in (x, y) coordinates. The picture of the flow that results is called the *phase portrait* of the flow in reference to the fact that, for the pendulum, a point in the phase portrait represents the instantaneous relation between the position and velocity of the pendulum. For what value of β can the "flow" defined by the phase portrait be used as a model of an incompressible fluid flow?

Problem 3 - Use (5.14) to reduce (5.12) to (5.15).

Problem 4 - Sketch the flow pattern generated by the 3-D linear system

$$\begin{aligned} \frac{dx}{dt} &= -y \\ \frac{dy}{dt} &= x \\ \frac{dz}{dt} &= z \end{aligned} \tag{5.53}$$

Work out the invariants of the velocity gradient tensor as well as the components of the rate-of-rotation and rate-of-strain tensors and vorticity vector. The vector field plotted in three dimensions is called the *phase space* of the system of ODEs.

In fluid mechanics the phase portrait or phase space is the physical space of the flow.

Problem 5 - Show that

$$S_{ij}A_{ji} = S_{ij}S_{ji} \tag{5.54}$$

and is therefore greater than or equal to zero.

Problem 6 - Work out the formulas for the components of the vorticity vector and show that the spin tensor is related to the vorticity vector by

$$W_{ik} = \frac{1}{2}\varepsilon_{ijk}\Omega_j . \tag{5.55}$$

Problem 7 - The velocity field given below has been used in the fluid mechanics literature to model a two dimensional separation bubble.

$$\begin{aligned} U(x, y) &= -y + 3y^2 + 3x^2y - (2/3)y^3 \\ V(x, y) &= -3xy^2 \end{aligned} \quad . \tag{5.56}$$

Draw the phase portrait and identify critical points.

Problem 8 - Consider the laminar flow near a 2-D separation point.

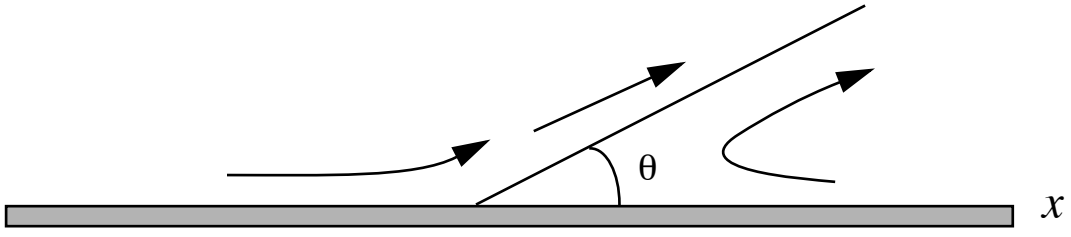

Use an expansion of the velocity field near the wall of the form

$$\begin{aligned} U &= a_{11}x + a_{12}y + b_{111}x^2 + b_{112}xy + b_{122}y^2 \\ V &= a_{21}x + a_{22}y + b_{211}x^2 + b_{212}xy + b_{222}y^2 \end{aligned} \quad . \tag{5.57}$$

Use the 2-D incompressible equations of motion and critical point theory to show that the angle of the separating streamline is

$$Tan(\theta) = -3\nu\frac{\Omega_x}{P_x} \tag{5.58}$$

where Ω_x and P_x are the x-derivatives of the vorticity and pressure at the wall. See Perry and Fairlie, Advances in Geophysics **B18**, 299, 1974 and Perry and Fairlie, Journal of Fluid Mechanics **Vol 69**, 657 1975 for a discussion of this problem and an experiment to study boundary layer separation and reattachment.